# Molecular Transport of Aliphatic Hydrocarbons Through Styrene Butadiene Rubber/Ethylene Vinyl Acetate Blends

**M. Padmini,[1] C. K. Radhakrishnan,[2] A. Sujith,[2] G. Unnikrishnan,[2] E. Purushothaman[3]**

[1]*Government Engineering College, Calicut 673 005, Kerala, India*
[2]*National Institute of Technology, Calicut 673 601, Kerala, India*
[3]*Department of Chemistry, University of Calicut, Malappuram 673635, Kerala, India*

Received 12 May 2005; accepted 1 October 2005
DOI 10.1002/app.23366
Published online in Wiley InterScience (www.interscience.wiley.com).

**ABSTRACT:** Polymer blends based on styrene butadiene rubber and ethylene vinyl acetate (EVA) were prepared. The sorption and diffusion of four aliphatic hydrocarbons through the blends were investigated with temperatures of 26–56°C. Sulfur, dicumyl peroxide (DCP), and a mixed system consisting of sulfur and DCP (mixed) were used as crosslinking agents for the blends. Of the three systems, the peroxide vulcanized blends were found to exhibit the lowest penetrant uptake. The aliphatic liquid penetration through the matrix decreased with an increase in the EVA content in the blends, which was attributed to the semicrystalline nature of the EVA matrix. The experimental observations were correlated with the morphology of the blends. Diffusion and permeation coefficients were calculated from the sorption data. A slight deviation from the Fickian trend was observed for the mechanism of transport with an increase in the EVA content in the blends. The molecular mass between crosslinks and thermodynamic parameters of sorption were determined from swelling data. The experimental observations were compared with different theoretical models.
 J Appl Polym Sci 101: 2884–2897, 2006

**Key words:** swelling; morphology; diffusion; crosslinking; blends

## INTRODUCTION

The importance of the examination of the diffusion and transport behavior of organic solvents through polymeric materials, which are used in a wide variety of engineering applications, has been widely recognized.[1–7] Solvent sorption and diffusion are the limiting factors of polymer end use applications because these processes change the mechanical properties and sometimes cause destruction in polymer structures. Polymer–polymer interactions can strongly influence the solvent sorption and transport properties of polymer blends. Comparing the interactions between the solvent and each of the pure polymers, consisting of the polymer blend, it is possible to obtain information about the interaction between the polymer components in the blends. A heterogeneous blend consists of a polymeric matrix in which the second polymer is embedded. Consequently, the effects of the permeability are very dependent on the degree of heterogeneity of the system and therefore on the method of preparation.[8]

Wang et al.[9] conducted diffusion experiments for xylene and toluene through different high-density polyethylene/modified polyamide blends at different temperatures. The results showed that the logarithm of the diffusion flux decreased linearly with the reciprocal of the temperature. Yamaguchi et al.[10] studied the transport mechanism of silver-containing solid-type carrier membranes, the humidity effect on the membrane conductance, water uptake, and benzene vapor transport. An $AgBF_4$/nafion blend membrane and silver-form nafion membrane were employed as the models for the salt/polymer blend membrane and ion exchange membrane, respectively. The $AgBF_4$/nafion blend membrane showed benzene selectivity over cyclohexane at low humidity. The effect of the humidity on the water uptake of the two types of membranes showed no serious difference. Kundu et al.[11] examined the solvent resistance, physical and flame retardancies, and dielectric properties of a blend of poly(ethylene vinyl acetate) and polychloroprene. The retention in tensile properties is maximum for polychloroprene in solvent aging and for poly(ethylene vinyl acetate) in air aging. Aminabhavi et al.[12] investigated the sorption and diffusion of *n*-alkanes and aliphatic hydrocarbons through ethylene–propylene random copolymer/isotactic polypropylene blends with a temperature interval of 25–70°C. Activation parameters for different transport processes and molar mass between crosslinks were evaluated

*Correspondence to:* G. Unnikrishnan (unnig@nitc.ac.in).
Contract grant sponsor: Council of Scientific and Industrial Research, New Delhi, India.

**TABLE I**
**Formulation of Mixes (phr)**

| Ingredient | Vulcanizing system | | |
|---|---|---|---|
| | Sulfur | DCP | Mixed |
| Polymer | 100.0 | 100.0 | 100.0 |
| Zinc oxide | 4.0 | | 4.0 |
| Stearic acid | 2.0 | | 2.0 |
| MBTS | 1.5 | — | 1.5 |
| Dicumyl peroxide (40% active) | — | 4.0 | 4.0 |
| Sulfur | 2.0 | — | 2.0 |

MBTS, mercaptobenzothiazyl disulfide.

and the results were used to discuss the polymer–solvent interactions. In addition, our research group conducted diffusion experiments using different macromolecular systems.[13–16]

The sorption and diffusion behavior of *n*-pentane, *n*-hexane, *n*-heptane, and *n*-octane through styrene butadiene rubber/ethylene vinyl acetate (SBR/EVA) blends in the temperature range of 26–56°C were examined in the present work, with special reference to the effects of the blend composition, nature of crosslinks, penetrant size, and temperature. Different kinetic and thermodynamic parameters were evaluated from the diffusion data. The experimental results were compared with various theoretical models.

## EXPERIMENTAL

The SBR used in this investigation, Syanoprene (SBR-1502), was manufactured by cold emulsion polymerization and was obtained from Korea Kumho Petro Chemicals Company Ltd. The EVA used was EVA-1802 obtained from National Organic Chemical Industries Ltd. (Mumbai, India). The additives sulfur, dicumyl peroxide (DCP), zinc oxide, stearic acid, and mercaptobenzothiazyl disulfide were commercial grade. The solvents *n*-pentane, *n*-hexane, *n*-heptane, and *n*-octane were obtained from E. Merck (India) Ltd. (Mumbai, India) with 99% initial purity. They were double distilled before use.

The blends of SBR/EVA with different blend ratios and crosslink systems were prepared on a two-roll

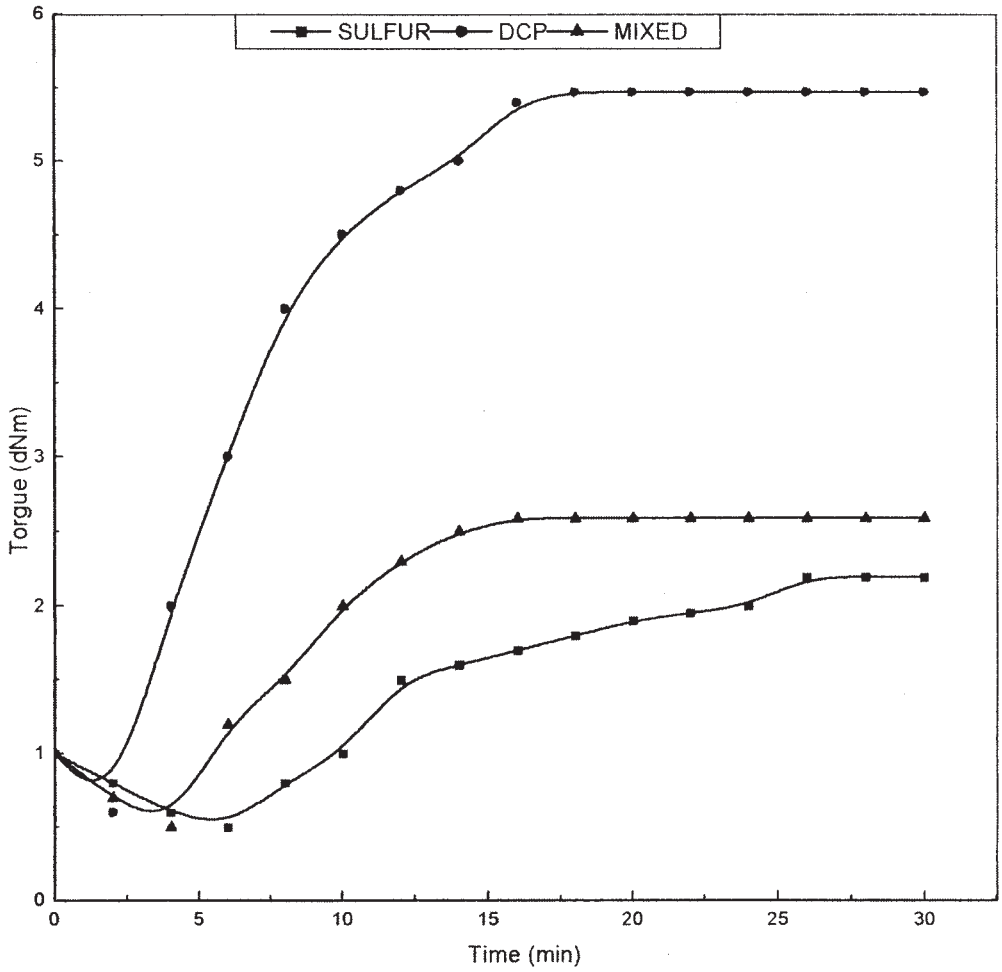


**Figure 1** Rheographs of 60/40 SBR/EVA with different crosslink systems.

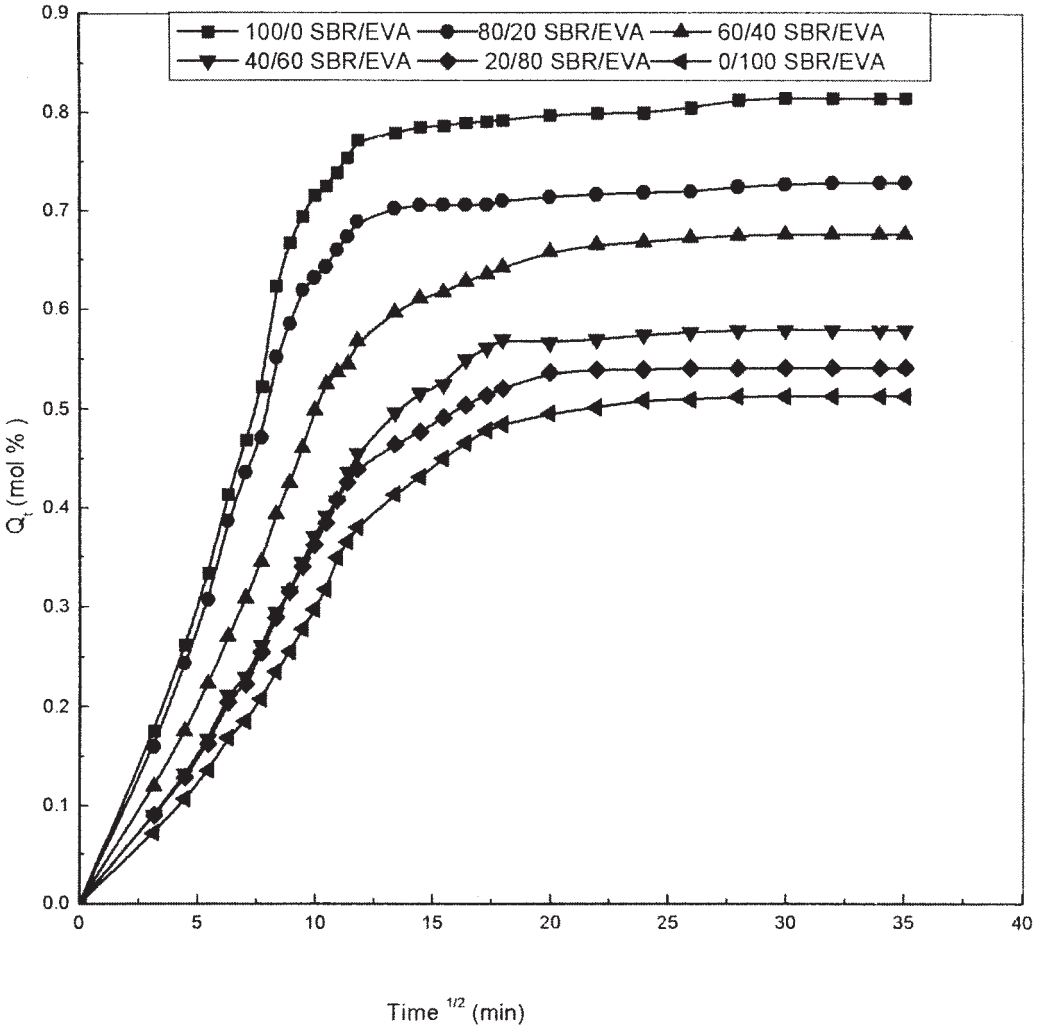


**Figure 2** The mole percentage uptake of hexane by different blend compositions crosslinked with DCP at 26°C.

mixing mill (150 × 300 mm) at a nip gap of 1.3 mm and a friction ratio of 1 : 1.4. The compounding formulations are given in Table I. The different crosslinking systems in the study were sulfur (S), peroxide (DCP), and mixed systems (S + DCP), which are indicated by S, DCP, and M, respectively. The curing behavior of the mixes was studied with a Monsanto Rheometer R-100 at a rotational frequency of 100 cycles/min. The rheographs of 60/40 SBR/EVA blends with different crosslink systems are given in Figure 1. The DCP vulcanized blend exhibits the highest torque, the sulfur system exhibits the lowest, and the mixed system is in between. The mixed cure system exhibits the longest cure time, and the peroxide cure system exhibits the lowest cure time. The curing of the samples was done on a hydraulic press at 160°C under a load of 30 tonnes.

For diffusion experiments, 1.9-cm diameter circular samples were punched out from the vulcanized sheets and dried overnight in a vacuum desiccator. The thickness of the samples was measured using a micrometer screw gauge with an accuracy of ±0.01 mm. The samples were immersed in stoppered test bottles kept in a thermostatically controlled air oven. The test samples were removed from the solvents at regular intervals; solvent adhered to the surface was rubbed off and weighed on a highly sensitive electronic balance (Shimadzu AW 210) that measured reproducibly within ±0.0001 g. They were then placed back into the test bottles. The process was continued until equilibrium swelling was achieved. To minimize the error due to the evaporation of the solvent from the samples, the weighing time was kept to a minimum of 30 s in all the experiments.[17] The results of the sorption experiments were expressed by plotting the mole percentage of uptake at time $t$ ($Q_t$) of the liquid by 100 g of the polymer blend against the square root of time. The value of $Q_t$ was calculated according to eq. (1):

$$Q_t = \frac{M_t/M_s}{M_p} \times 100 \quad (1)$$

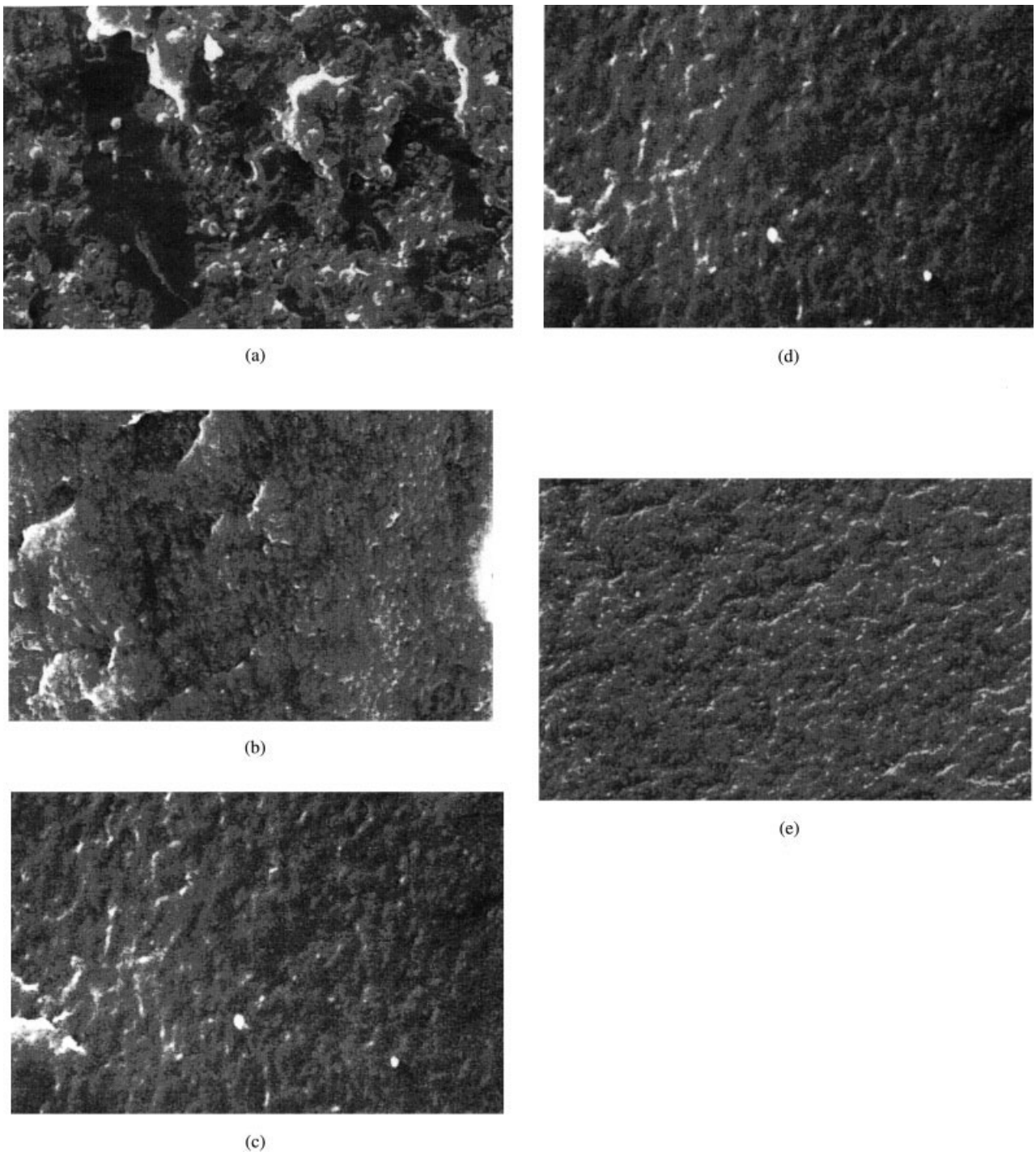


**Figure 3** Scanning electron micrographs of the (a) 60/40 SBR/EVA sulfur system, (b) 40/60 SBR/EVA sulfur system, (c) 20/80 SBR/EVA sulfur system, (d) 40/60 SBR/EVA mixed system, and (e) 40/60 SBR/EVA DCP system.

where $M_t$ is the mass of the solvent absorbed at a given time, $M_s$ is the molecular mass of the solvent, and $M_p$ is the mass of the polymer blend.

## RESULTS AND DISCUSSION

Figure 2 shows the liquid sorption behavior of SBR/EVA blend systems vulcanized by DCP at 26°C. The penetrant used was hexane. The graph clearly shows that pure EVA has the lowest equilibrium uptake and, upon blending with SBR, the $Q_t$ values regularly increase. Pure EVA is semicrystalline in nature. When blended with SBR, the crystalline regions of EVA become disrupted. The reduction in crystallinity makes the matrix absorb more solvent molecules. The tendency regularly increases with the increase in SBR

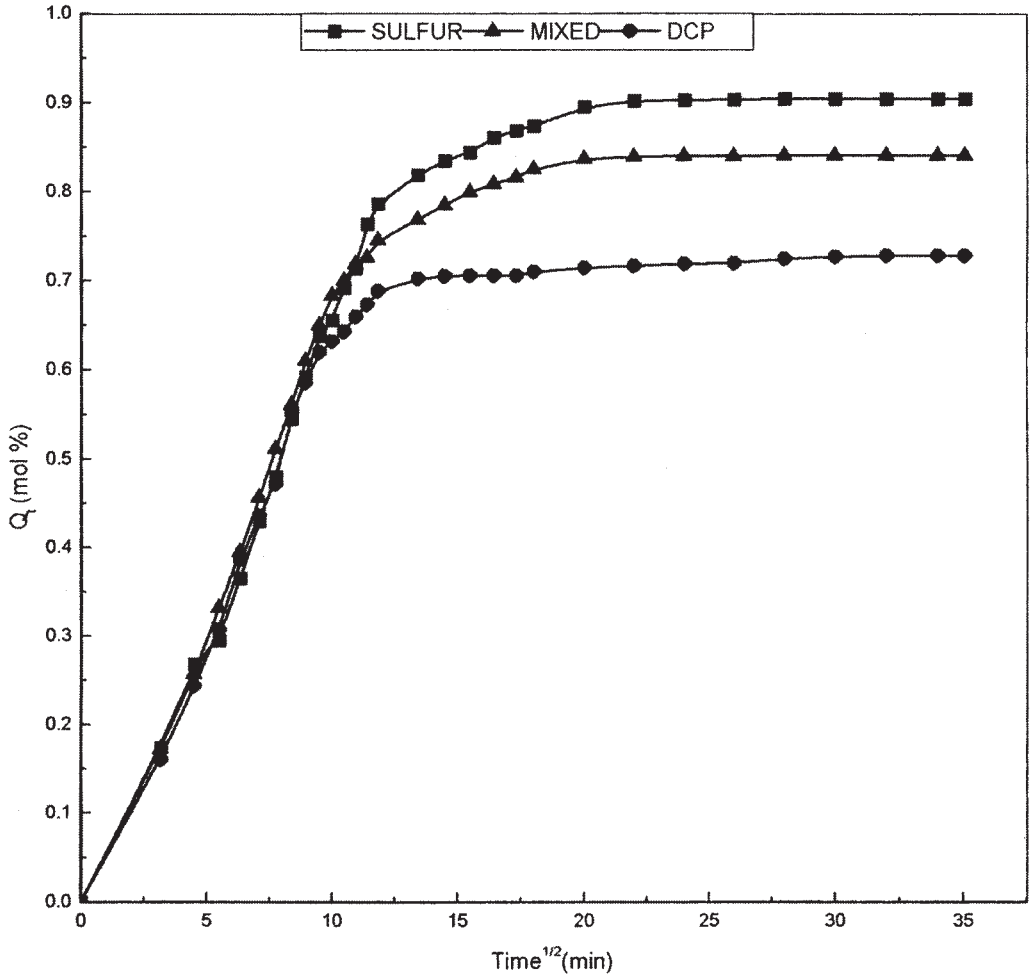


**Figure 4** The mole percentage uptake of hexane by 80/20 SBR/EVA with different crosslinking systems at 260°C.

content in the polymer blends. Figure 3(a) shows the SEM photographs of the sulfur vulcanized 60/40 SBR/EVA blend. The EVA particles are dispersed as domains in the continuous SBR matrix. Figure 3(b,c) shows the change in phase morphology of the blends upon increasing the EVA content to 60 and 80%, respectively. The domain size of the dispersed phase was found to decrease and the blend attained a cocontinuous morphology from the samples with 60–80% EVA. It is clear from the SEM photographs that the free volume of the blends decreases with an increase in EVA content, which contributes to the decrease in diffusion of the solvents through the blends with higher EVA content.

Figure 4 shows the sorption curves of 80/20 SBR/EVA crosslinked with three vulcanizing systems, namely, sulfur, DCP, and the mixed systems. The solvent used was hexane, and the experiments were conducted at 26°C. It is clear from the figure that the SBR/EVA crosslinked with sulfur system absorbs the highest amount of the liquid, whereas that crosslinked with the DCP system takes up the lowest amount. The difference in the maximum uptake values of SBR/EVA with different crosslinking systems may be due to the different types of crosslinks present in them.[13] The sulfur vulcanization introduces flexible polysulfidic linkages between the macromolecular chains. This allows the easy accommodation of penetrant molecules within the matrix. The bond lengths and bond energies given in Table II also support this view. The DCP vulcanized system has only stable C—C linkages and consequently shows the lowest $Q_t$ values. The same trend was observed with pentane and octane for

**TABLE II**
**Bond Length and Bond Energies of Different Types of Chemical Linkages**

| Type of bond | Bond length (nm) | Bond energy (kJ/mol) |
|---|---|---|
| C—C | 0.154 | 355 |
| C—S | 0.181 | 267 |
| S—S | 0.188 | 238 |

**TABLE III**
**Values of Interaction Parameter**

| SBR/EVA | Temp. (°C) | $\chi$ | | | |
|---|---|---|---|---|---|
| | | Pentane | Hexane | Heptane | Octane |
| 100/0 | 26 | 0.8366 | 0.7113 | 0.7001 | 0.6129 |
| | 36 | | 0.6992 | 0.6885 | 0.6041 |
| | 46 | | 0.6879 | 0.6775 | 0.5958 |
| | 56 | | 0.6773 | 0.6672 | 0.5881 |
| 80/20 | 26 | 0.8875 | 0.7584 | 0.7497 | 0.6583 |
| | 36 | | 0.7448 | 0.7365 | 0.6480 |
| | 46 | | 0.7321 | 0.7240 | 0.6384 |
| | 56 | | 0.7200 | 0.7122 | 0.6294 |
| 60/40 | 26 | 0.9409 | 0.8077 | 0.8026 | 0.7072 |
| | 36 | | 0.7931 | 0.7876 | 0.6954 |
| | 46 | | 0.7788 | 0.7735 | 0.6842 |
| | 56 | | 0.7655 | 0.7602 | 0.6738 |
| 40/60 | 26 | 0.9896 | 0.8543 | 0.8514 | 0.7529 |
| | 36 | | 0.8376 | 0.8349 | 0.7395 |
| | 46 | | 0.8219 | 0.8193 | 0.7269 |
| | 56 | | 0.8072 | 0.8046 | 0.7153 |
| 20/80 | 26 | 1.0477 | 0.9095 | 0.9102 | 0.8083 |
| | 36 | | 0.8909 | 0.8918 | 0.7932 |
| | 46 | | 0.8736 | 0.8744 | 0.7789 |
| | 56 | | 0.8574 | 0.8580 | 0.7658 |
| 0/100 | 26 | 1.1083 | 0.9675 | 0.9723 | 0.8673 |
| | 36 | | 0.9471 | 0.9518 | 0.8503 |
| | 46 | | 0.9280 | 0.9326 | 0.8342 |
| | 56 | | 0.9101 | 0.9144 | 0.8194 |

all blend ratios at temperatures of 36, 46, and 56°C. Figure 3(b,d,e) shows a comparison of the phase morphology of 40/60 SBR/EVA blends vulcanized by sulfur, mixed, and DCP systems, respectively. It is evident from the photographs that a fine and more uniform phase distribution is exhibited by the DCP vulcanized samples. The domain size of the dispersed phase was found to decrease in the order sulfur > mixed > DCP. Thus, the observed solvent uptake behavior of the blends with different vulcanizing systems was in good agreement with the morphology.

In order to find out how well the observed solvent uptake behavior correlates with the crosslink distribution in the matrix, we calculated the molecular mass between crosslinks ($M_c$) using the Flory–Rehner equation:[18]

**TABLE IV**
**Values of Molar Mass Between Crosslinks ($M_c$)**

| SBR/EVA | Vulcanizing system | $M_c$ (g/mol) | | | |
|---|---|---|---|---|---|
| | | Pentane | Hexane | Heptane | Octane |
| 100/0 | Sulfur | 4,379 | 8,563 | 1,650 | 36,215 |
| | Mixed | 3,663 | 5,239 | 1,601 | 25,691 |
| | DCP | 3,566 | 3,935 | 1,456 | 25,066 |
| 80/20 | Sulfur | 2,648 | 3,544 | 1,366 | 27,676 |
| | Mixed | 2,045 | 2,866 | 1,258 | 13,136 |
| | DCP | 1,824 | 2,003 | 1,098 | 4,891 |
| 60/40 | Sulfur | 830 | 1,320 | 825 | 4,873 |
| | Mixed | 810 | 1,220 | 804 | 4,672 |
| | DCP | 801 | 1,134 | 770 | 3,144 |
| 40/60 | Sulfur | 723 | 881 | 567 | 4,129 |
| | Mixed | 769 | 834 | 713 | 3,711 |
| | DCP | 696 | 792 | 680 | 2,882 |
| 20/80 | Sulfur | 653 | 804 | 649 | 3,772 |
| | Mixed | 641 | 766 | 575 | 1,954 |
| | DCP | 562 | 635 | 326 | 1,285 |
| 0/100 | DCP | 535 | 586 | 308 | 1,019 |

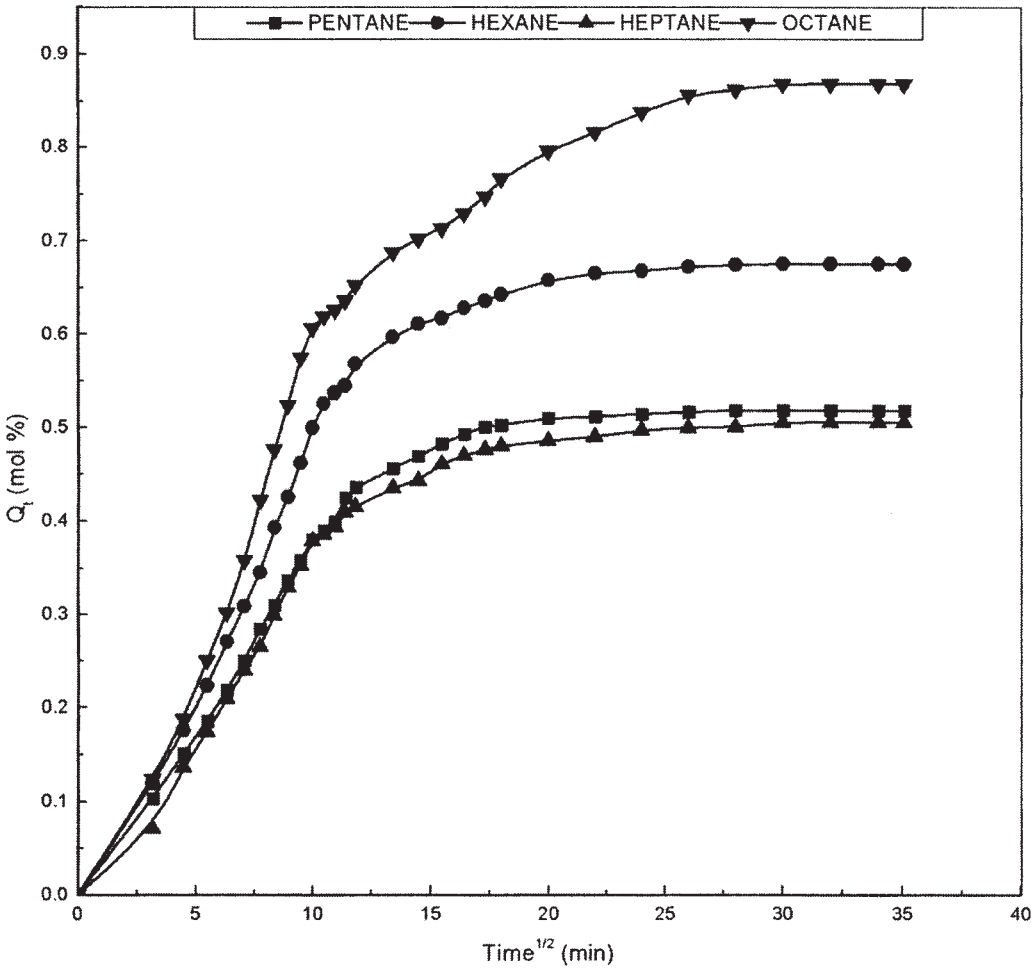


**Figure 5** The mole percentage uptake of DCP crosslinked 60/40 SBR/EVA in pentane, hexane, heptane, and octane.

$$M_c = \frac{-\rho_p V \phi^{1/3}}{[ln(1-\phi) + \phi\chi\phi^2]} \quad (2)$$

where $\rho_p$ is the density of the matrix, $V$ is the molar volume of the solvent, $\phi$ is the volume fraction of the polymer blend in the fully swollen state, and $\chi$ is the blend–solvent interaction parameter computed from the Flory–Huggins theory of dilute polymer solutions,[19]

$$\chi = \beta + V_s/RT(\delta_s - \delta_p)^2 \quad (3)$$

where $\delta_s$ and $\delta_p$ are the solubility parameters of the solvent and the polymer, respectively; $\beta$ is a lattice constant whose value is generally taken to be 0.34 for elastomer–solvent systems; $R$ is the universal gas constant; and $T$ is the temperature on the absolute scale. The $\chi$ values for different blend systems vulcanized by sulfur in different solvents at ambient and at higher temperatures are shown in Table III. It is interesting to note that the $\chi$ values increase with increases in EVA content in the blends and decrease with increases in temperature. Lower values of $\chi$ indicate higher polymer solvent interaction.

The values of $M_c$ for different blend systems in different solvents are given in Table IV. We observed that there is a regular decrease in the $M_c$ values with increases in the EVA content. With respect to the crosslink systems, the order sulfur > mixed > DCP is maintained. These observations are in good agreement with the observed effects of the blend ratio and the penetrant size. However, it is interesting to note the changes in the $M_c$ values for a given blend ratio and crosslinking system with the change of penetrants. These can be explained by distinguishing between the apparent concentration of physical crosslinks ($X_{(phy)}$) and the concentration of chemically discrete crosslinks ($X_{(che)}$) that result directly from vulcanization. The physical and chemical effects are additive and $X_{phy} = X_{che} + X_{int}$, where $X_{int}$ is the initial crosslink density due to entanglement, constraints, or other effects attributable to chemical changes. Because the rubber chain entanglements can be different in different solvents, the $M_c$ values ob-

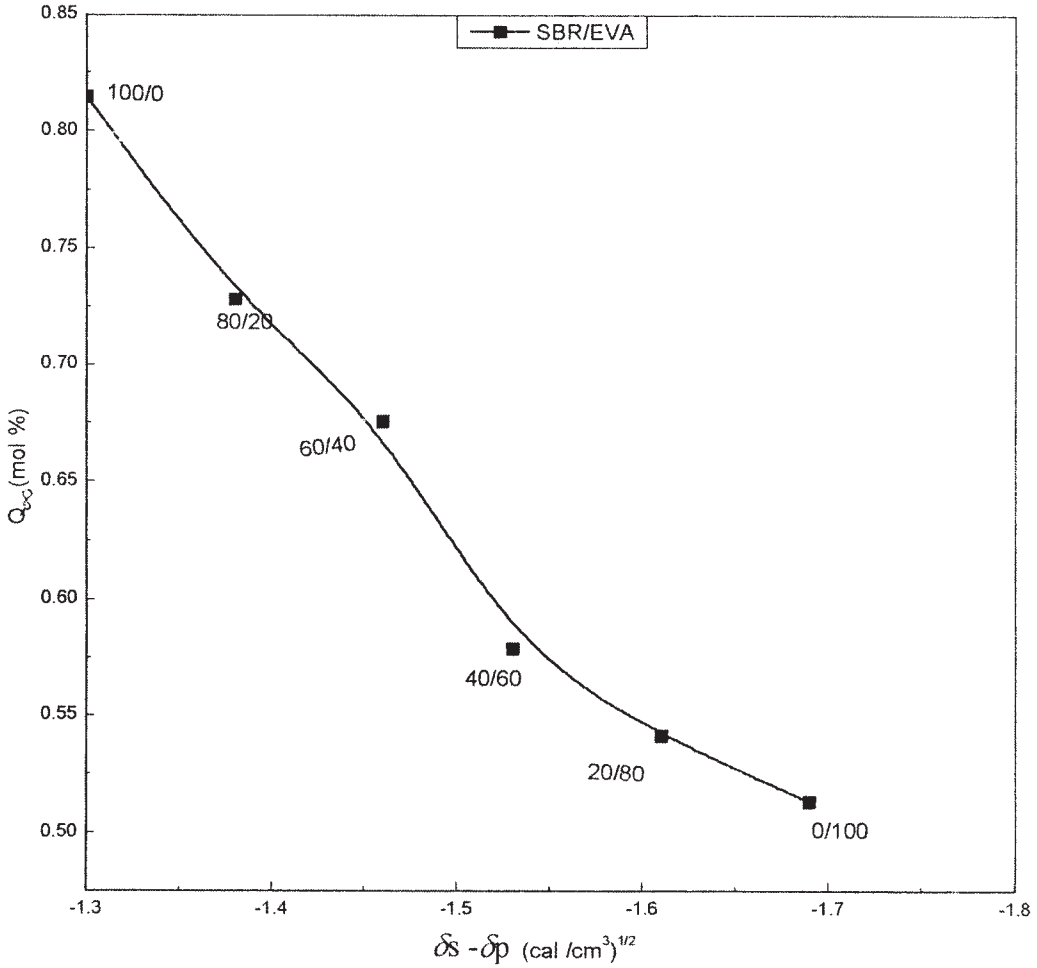


**Figure 6** The variation of the $Q_\infty$ with $\delta_s - \delta_p$ values for the SBR/EVA blend in hexane.

tained from the Flory–Rehner theory applied to a series of rubber–solvent systems can be regarded as physical crosslinks. The changes in the rubber chain entanglement density in different solvents is probably the reason for the variation of the $M_c$ values with the change of solvent.[15]

**TABLE V**
**Values of *n* and *k***

| SBR/EVA | Vulcanizing system | *n* | | | | $k \times 10^2$ (g/g min$^2$) | | | |
|---|---|---|---|---|---|---|---|---|---|
| | | Pentane | Hexane | Heptane | Octane | Pentane | Hexane | Heptane | Octane |
| 100/0 | Sulfur | 0.54 | 0.61 | 0.62 | 0.65 | 10.13 | 4.99 | 4.84 | 4.40 |
| | Mixed | 0.50 | 0.59 | 0.59 | 0.63 | 10.04 | 5.69 | 4.77 | 3.19 |
| | DCP | 0.52 | 0.63 | 0.59 | 0.69 | 12.87 | 4.86 | 5.48 | 3.69 |
| 80/20 | Sulfur | 0.55 | 0.59 | 0.66 | 0.66 | 6.54 | 4.78 | 3.55 | 3.34 |
| | Mixed | 0.55 | 0.61 | 0.61 | 0.66 | 6.32 | 5.03 | 4.78 | 3.85 |
| | DCP | 0.56 | 0.62 | 0.60 | 0.69 | 6.23 | 5.27 | 5.03 | 3.46 |
| 60/40 | Sulfur | 0.58 | 0.62 | 0.65 | 0.63 | 5.44 | 4.51 | 3.79 | 4.13 |
| | Mixed | 0.61 | 0.61 | 0.60 | 0.68 | 5.35 | 4.85 | 4.59 | 3.29 |
| | DCP | 0.57 | 0.62 | 0.69 | 0.61 | 5.23 | 4.04 | 2.99 | 2.64 |
| 40/60 | Sulfur | 0.58 | 0.56 | 0.63 | 0.66 | 5.44 | 5.78 | 3.65 | 3.36 |
| | Mixed | 0.63 | 0.62 | 0.59 | 0.66 | 3.85 | 4.45 | 5.09 | 2.98 |
| | DCP | 0.57 | 0.62 | 0.59 | 0.66 | 4.50 | 3.61 | 3.82 | 3.21 |
| 20/80 | Sulfur | 0.59 | 0.58 | 0.62 | 0.65 | 3.35 | 5.28 | 3.25 | 3.13 |
| | Mixed | 0.69 | 0.60 | 0.58 | 0.62 | 2.62 | 4.18 | 4.34 | 2.91 |
| | DCP | 0.55 | 0.62 | 0.61 | 0.69 | 6.05 | 3.83 | 4.03 | 2.57 |
| 0/100 | DCP | 0.72 | 0.71 | 0.76 | 0.78 | 4.15 | 3.47 | 4.14 | 4.09 |

**TABLE VI**
**Values of Diffusion and Permeation Coefficients at 26°C**

| SBR/EVA | Vulcanizing system | $D^* \times 10^4$ (cm$^2$/s) | | | | $P \times 10^4$ (cm$^2$/s) | | | |
|---|---|---|---|---|---|---|---|---|---|
| | | Pentane | Hexane | Heptane | Octane | Pentane | Hexane | Heptane | Octane |
| 100/0 | Sulfur | 2.98 | 6.65 | 4.78 | 45.62 | 1.89 | 6.69 | 4.45 | 100.72 |
| | Mixed | 2.55 | 4.42 | 3.51 | 18.06 | 1.51 | 3.87 | 2.89 | 30.80 |
| | DCP | 1.63 | 4.16 | 2.19 | 8.52 | 0.86 | 2.90 | 1.45 | 9.85 |
| 80/20 | Sulfur | 2.19 | 3.39 | 2.78 | 19.26 | 1.22 | 2.64 | 2.30 | 32.28 |
| | Mixed | 1.65 | 2.91 | 2.12 | 17.32 | 0.80 | 2.10 | 1.40 | 24.96 |
| | DCP | 1.42 | 2.66 | 1.80 | 5.94 | 0.68 | 1.66 | 1.03 | 6.25 |
| 60/40 | Sulfur | 1.77 | 2.77 | 2.04 | 8.45 | 0.76 | 1.67 | 1.09 | 9.81 |
| | Mixed | 1.51 | 1.96 | 1.52 | 6.67 | 0.67 | 1.23 | 0.78 | 6.51 |
| | DCP | 0.98 | 1.93 | 1.25 | 4.74 | 0.37 | 1.13 | 0.67 | 4.79 |
| 40/60 | Sulfur | 1.65 | 1.53 | 0.91 | 3.50 | 0.63 | 0.81 | 0.54 | 3.14 |
| | Mixed | 0.96 | 1.47 | 0.86 | 2.84 | 0.32 | 0.73 | 0.38 | 2.84 |
| | DCP | 0.72 | 1.21 | 0.76 | 2.66 | 0.28 | 0.61 | 0.37 | 2.19 |
| 20/80 | Sulfur | 1.42 | 1.23 | 0.76 | 2.60 | 0.52 | 0.63 | 0.31 | 3.05 |
| | Mixed | 0.62 | 1.02 | 0.72 | 2.39 | 0.15 | 0.48 | 0.22 | 1.92 |
| | DCP | 0.52 | 0.94 | 0.59 | 1.25 | 0.13 | 0.41 | 0.21 | 0.95 |
| 0/100 | DCP | 0.50 | 0.82 | 0.49 | 0.94 | 0.17 | 0.36 | 0.15 | 1.81 |

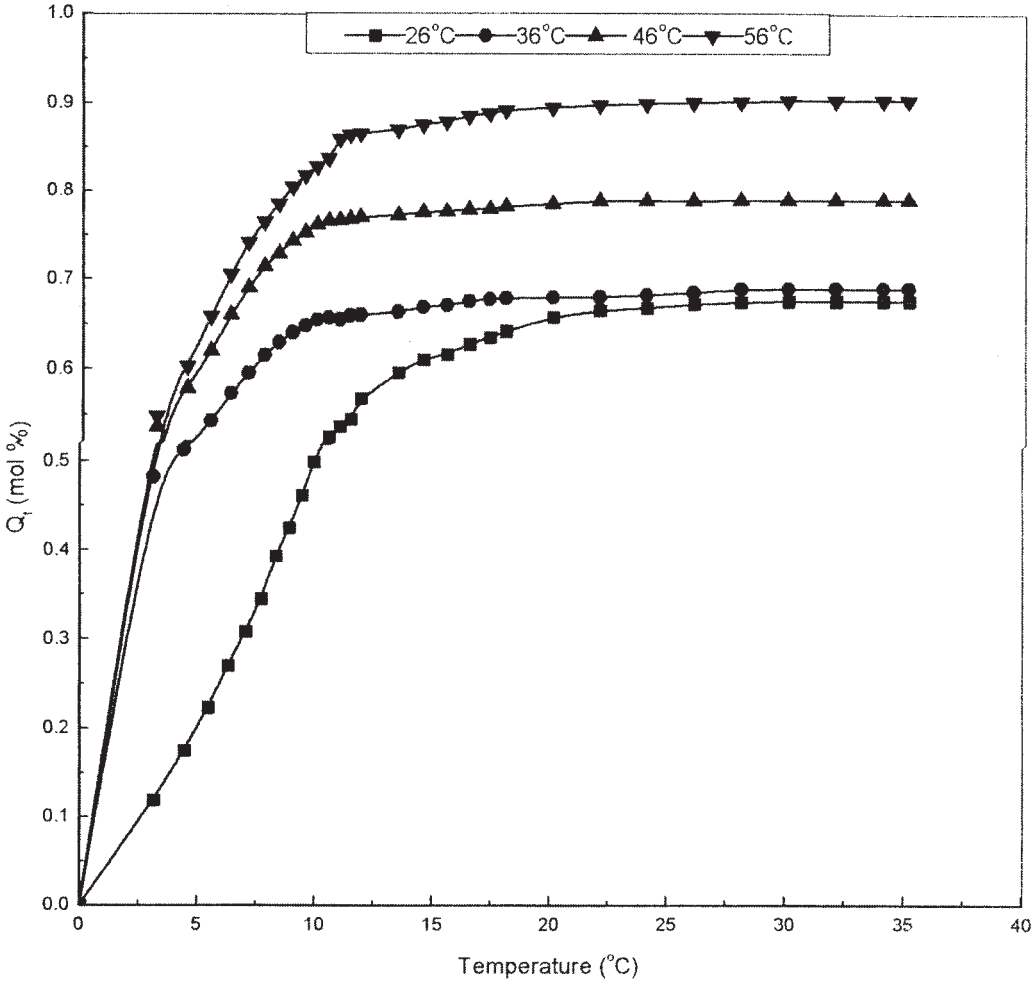


**Figure 7** The temperature dependence of the DCP vulcanized 60/40 SBR/EVA blend in hexane.

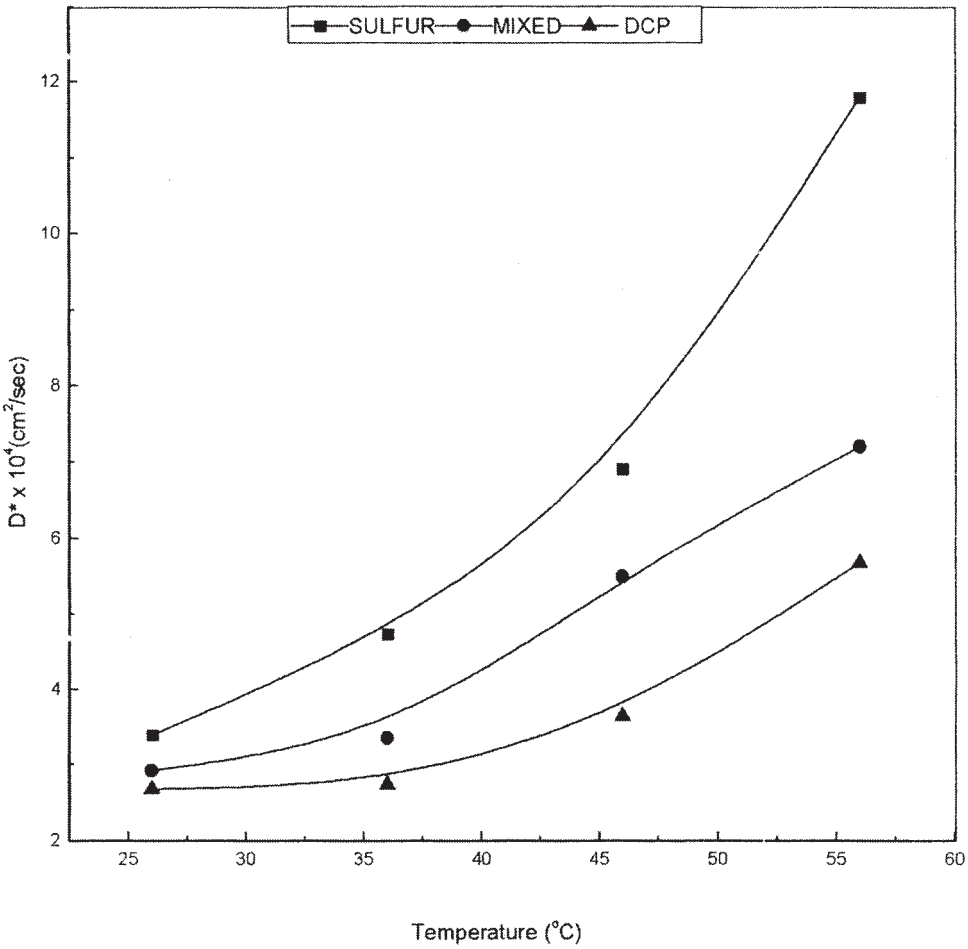


**Figure 8** The variation of the $D^*$ values with the temperature for the 80/20 SBR/EVA blend with different crosslinked systems in hexane.

Figure 5 shows the effect of the penetrant size on the sorption and diffusion of four aliphatic hydrocarbons through the peroxide systems. It follows from the graph that the trend is in the order octane > hexane > pentane > heptane. Note that the observation is in the reverse order of the normal effect of the molecular mass of the solvent on transport, with the exception of heptane, which shows lower mole percentage increase at equilibrium ($Q_\infty$) values than expected. Such anomalous results were reported earlier as well.[20] The permeation through any matrix is a combination of sorption and diffusion. The kinetics of diffusion depends on the molecular mass of the solvent whereas sorption depends on the difference in the solubility parameter values. The highest uptake exhibited by octane is due to the dominance of the solubility parameter over the molecular mass of the solvent during transport. The smaller the difference, the greater is the affinity of a polymer toward the solvent. The difference in the solubility parameters of the solvent and the polymer blend ($\delta_s - \delta_p$) is plotted against the equilibrium sorption values in Figure 6, which shows that as ($\delta_s - \delta_p$) increases, the equilibrium sorption value decreases.

In order to find the mechanism of the transport phenomenon, the dynamic swelling data were fitted to the equation[17]

**TABLE VII**
**Values of Activation Energy**

| SBR/EVA | Vulcanizing system | $E_D$ (kJ/mol) Hexane | Heptane |
|---|---|---|---|
| 100/0 | Sulfur | 1.07 | 8.58 |
| | Mixed | 5.24 | 8.99 |
| | DCP | 6.96 | 13.85 |
| 80/20 | Sulfur | 44.66 | 47.63 |
| | Mixed | 22.61 | 32.85 |
| | DCP | 21.24 | 25.10 |
| 60/40 | Sulfur | 69.33 | 58.77 |
| | Mixed | 39.16 | 53.08 |
| | DCP | 39.26 | 42.22 |
| 40/60 | Sulfur | 94.79 | 77.32 |
| | Mixed | 55.26 | 62.55 |
| | DCP | 75.81 | 77.02 |
| 20/80 | Sulfur | 105.41 | 98.47 |
| | Mixed | 72.35 | 93.51 |
| | DCP | 121.64 | 101.86 |
| 0/100 | DCP | 124.36 | 132.51 |

**TABLE VIII**
**Values of $\Delta S$ and $\Delta H_s$**

| SBR/EVA | Vulcanizing system | $\Delta H_s$ (kJ/mol) | | $\Delta S$ (J/mol/K) | |
|---|---|---|---|---|---|
| | | Hexane | Heptane | Hexane | Heptane |
| 100/0 | Sulfur | −0.068 | 0.047 | −2.177 | −1.876 |
| | Mixed | −0.079 | 0.166 | −2.268 | −2.268 |
| | DCP | −0.084 | 0.038 | −2.379 | −1.962 |
| 80/20 | Sulfur | 0.728 | 0.993 | 0.354 | 1.118 |
| | Mixed | 0.339 | 0.575 | −0.922 | −0.329 |
| | DCP | 0.566 | 0.582 | −0.278 | −0.251 |
| 60/40 | Sulfur | 1.132 | 1.287 | 1.579 | 1.991 |
| | Mixed | 0.601 | 0.939 | −0.109 | 0.801 |
| | DCP | 0.711 | 1.111 | 0.15 | 1.407 |
| 40/60 | Sulfur | 1.595 | 1.605 | 3.039 | 2.944 |
| | Mixed | 0.931 | 1.65 | 0.934 | 3.092 |
| | DCP | 1.357 | 1.715 | 2.241 | 3.323 |
| 20/80 | Sulfur | 1.98 | 2.16 | 3.842 | 4.32 |
| | Mixed | 2.39 | 3.063 | 5.665 | 7.849 |
| | DCP | 2.13 | 1.895 | 4.792 | 3.842 |
| 100/0 | DCP | 3.47 | 0.69 | 6.10 | 1.32 |

$$log\ Q_t/Q_\infty = \log k + n \log t \tag{4}$$

Here, $k$ is a constant that depends on the structural characteristics of the polymer blend in addition to its interaction with the solvent. The magnitude of $n$ denotes the transport mode. When $n = 1$, the diffusion mechanism is said to be non-Fickian and the rate of relaxation of the polymer chain is slower than the solvent diffusion. If the value lies between 1 and 0.5, the mechanism is said to follow an anomalous trend where the polymer chain relaxation rate and the solvent diffusion rate are similar. The values of $n$ and $k$ are given in Table V. The $n$ values indicate that the mechanism of transport slightly deviates from the normal Fickian behavior observed for conventional elastomers.

The diffusivity ($D$) of the blend–solvent systems was calculated using the equation[21]

$$D = \pi(h\theta/4Q_\infty)^2 \tag{5}$$

where $\theta$ is the slope of the diffusion curves before attaining 50% of the equilibrium, $h$ is the initial thickness of the sample, and $Q_\infty$ is the mole percentage increase in the solvent uptake at equilibrium. A correction to the diffusion coefficients under swollen conditions was found to be essential because significant swelling was observed during sorption experiments in all the solvents. This was done by calculating the intrinsic diffusion coefficient ($D^*$) from the volume fraction ($\phi$) of the polymer blend samples using the expression[22]

$$D^* = \frac{D}{\phi^{7/3}} \tag{6}$$

The estimated values of the intrinsic diffusion coefficients are given in Table VI. The $D^*$ values depend on the nature of the crosslinks, temperature, and penetrant size. It has been found that the $D^*$ values are highest for the sulfur system and lowest for the DCP system in a given penetrant. These observations are in good agreement with the decrease in the values of the sorption equilibrium in the order sulfur > mixed > DCP.

The permeation coefficient for all the systems under investigation was calculated by the equation[23]

$$P = D^*S \tag{7}$$

The values of $P$ are also given in Table VI. We can see that the trend is the same as that of the $D^*$ values.

To study the effect of temperature, we also conducted experiments at 36, 46, and 56°C in addition to those at 26°C. Figure 7 shows the temperature dependence of the peroxide system 80/20 SBR/EVA in hexane. The rate of diffusion and the maximum uptake ($Q_\infty$) were found to increase with the temperature. The variation of the $D^*$ values with temperature is shown in Figure 8. The solvent used was hexane. It shows that $D^*$ values increase with the temperature. The values of $D^*$ at different temperatures were used to estimate the activation energy for transport from the Arrhenius-type relation[24]

$$\log D^* = \log D_0^* - \frac{E_D}{2.303RT} \tag{8}$$

where $D_o^*$ is the pre-exponential factor; $R$, the universal gas constant. $T$ and $E_D$ are the temperature on the absolute scale and activation energy, respectively. Typical Arrhenius plot of log $D^*$ versus $1/T$ is given in Figure 9. It is interesting to note that at 46°C and 56°C, the $D^*$ values show a reverse trend with respect to the

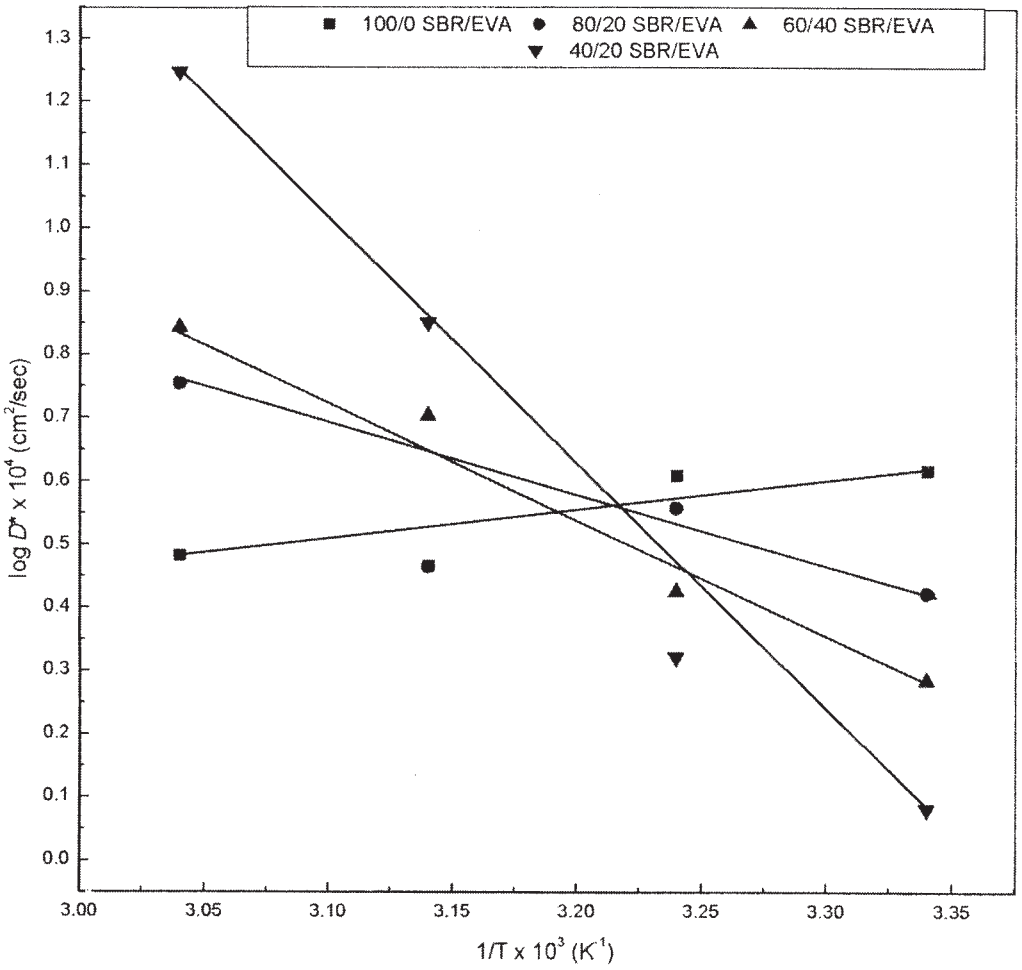


**Figure 9** An Arrhenius plot of the different blend systems of DCP crosslinked in hexane.

blend ratio. It can be explained on the basis of the effect of temperature on the crystallinity of EVA. At higher temperatures, higher EVA content samples lose their crystallinity and become more flexible than SBR. This results in the non-tortuous movement of the solvents through the matrix. Because of this, the higher EVA content samples show highest solvent uptake at higher temperature. The calculated values of $E_D$ for the solvent hexane and heptane are given in Table 7. It is found that the activation energy values increase with increase in EVA content in the blends.

From the amount of penetrant sorbed by a given mass of the polymer blend, the equilibrium sorption constant ($K_s$) was computed as follows:

$$K_s = \frac{\text{number of moles of solvent sorbed at equilibrium}}{\text{mass of polymer blend}} \tag{9}$$

From the value of $K_s$ it is possible to calculate the enthalpy change ($\Delta H_s$) and entropy change ($\Delta S$) using the Van't Hoff relation[25]

$$\log K_s = \frac{\Delta S}{2.303R} - \frac{\Delta H_s}{2.303RT} \tag{10}$$

The values of $\Delta H_s$ and $\Delta S$ for hexane and heptane are given in Table VIII. Most of the $\Delta H_s$ values are found to be positive, which suggests that the sorption process is endothermic in this case.

Polymer blends involve domains that are rich in one of the polymeric species confined in a continuous matrix that is rich in the second polymeric component. It is interesting to interpret the permeability of heterogeneous blends through theoretical models. Robeson's two limiting models (series and parallel models) are generally used in the case of polymer blends.[8]

According to the parallel model,

$$P_c = P_1\phi_1 + P_2\phi_2 \tag{11}$$

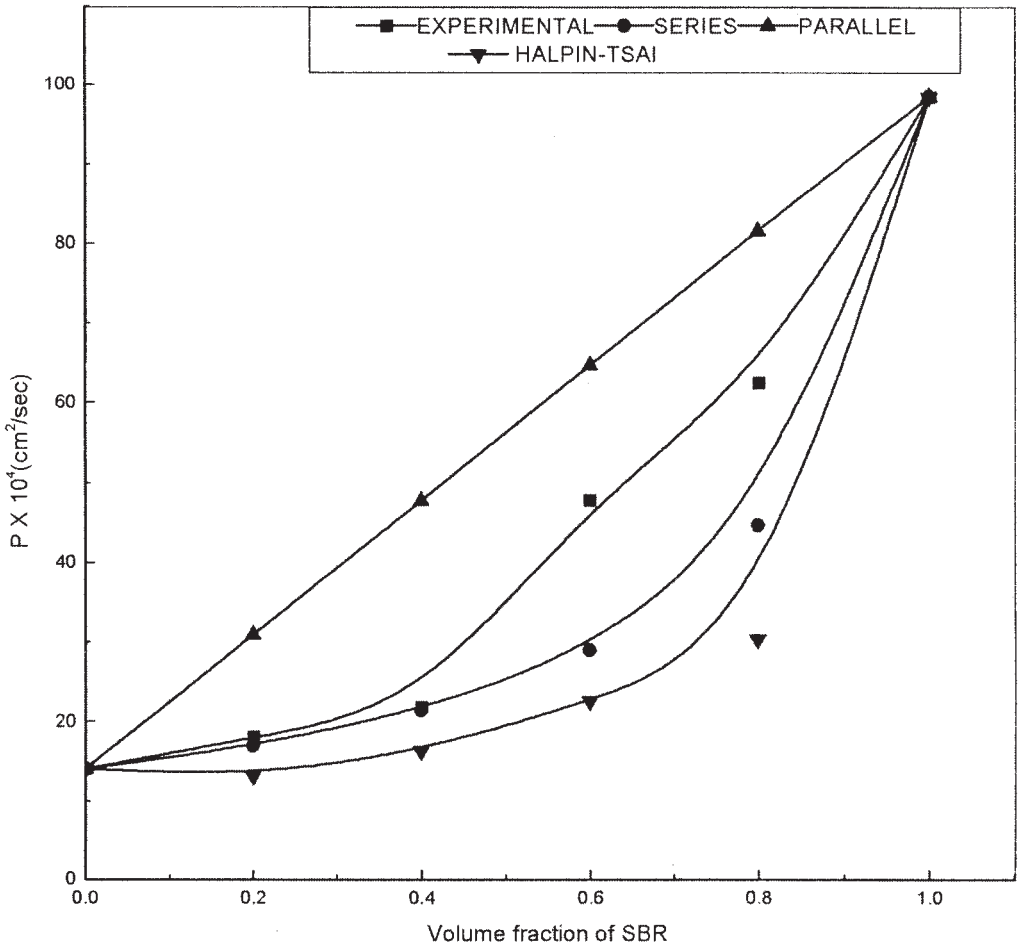


**Figure 10** Curves showing the variation of the permeability coefficient with the volume fraction of SBR in the blends vulcanized with DCP.

By the series model,

$$P_c = P_1P_2/(\phi_1P_2 + \phi_2P_1) \quad (12)$$

where $P_c$, $P_1$, and $P_2$ are the permeation coefficients of the blend, component I, and component II, respectively; and $\phi_1$ and $\phi_2$ are the volume fractions of components I and II, respectively.

Another model that can be applied is the Halpin–Tsai equation,[26]

$$P_1/P_c = (1 + A_iB_i\phi_2)/(1 - B_i\phi_2) \quad (13)$$

where

$$B_i = (P_1/P_2 - 1)/(P_1/P_2 + A_i) \quad (14)$$

In these equations subscripts 1and 2 refer to the continuous and dispersed phases, respectively, and the constant $A_i$ is defined by the morphology of the system. When an elastomer forms the dispersed phase in the continuous hard matrix, $A_i = 0.66$. When the hard material forms the dispersed phase in a continuous elastomer matrix, then $A_i = 1.5$. Figure 10 shows the variation of the permeability coefficient with the volume fraction of SBR in the blends vulcanized with DCP. The experimental curve was found to be closer to the series model for transport.

## CONCLUSION

The transport characteristics of SBR/EVA blends with different vulcanizing systems were studied using *n*-pentane, *n*-hexane, *n*-heptane, and *n*-octane as penetrants in a temperature range of 26–56°C, with special reference to the effects of the blend ratio, crosslinking systems, penetrant size, and temperature. The regular reduction in solvent uptake by the blends with increases in EVA content were attributed to the semicrystalline nature of EVA. The sample crosslinked by DCP showed the lowest equilibrium uptake in all penetrants compared to the samples with sulfur and mixed vulcanization modes. This was explained in terms of the differences in the nature and distribution of crosslinks in the network. The calculated $M_c$

values complement the observation for the equilibrium uptake values. The interaction parameter values decrease with increases in EVA content and temperature. The solvent uptake follows the order octane > hexane > pentane > heptane for a given blend system. The highest uptake exhibited by octane is attributable to the dominance of the solubility parameter over the molecular mass of the solvent during transport. The diffusion and permeation coefficient values decrease with increases in EVA content in the blends. Thermodynamic parameters such as the enthalpy and entropy were determined using the Van't Hoff relationship. Different diffusion models were applied to analyze the transport data, and the results were found to be closer to the series model.

The corresponding author (G.U.) acknowledges the financial support from the Council of Scientific and Industrial Research, New Delhi, India.

## References

1. Dixon-Garrett, S. V.; Nagai, K.; Freeman, B. D. J Polym Sci Part B: Polym Phys 2000, 38, 1078.
2. Vergnaud, J. M. Liquid Transport Process in Polymeric Materials—Modeling and Industrial Applications; Prentice–Hall: Englewood Cliffs, NJ, 1991.
3. Huang, R. Y. M. Pervaporation Membrane Separation Process; Elsevier: Amsterdam, 1991.
4. Wiberg, G.; Hedenqvist, M. S.; Boyd, R. H.; Gedde, U. W. Polym Eng Sci 1998, 38, 1640.
5. Freeman, B. D.; Pinnau, I. In Polymeric Membranes for Gas and Vapour Separations: Chemistry and Material Science; Freeman, B. D.; Pinnau, I., Eds.; ACS Symposium Series 733; American Chemical Society: Washington, DC, 1999; p 1.
6. Schlick, S.; Gao, Z.; Matsukawa, S.; Ando, I.; Fred, E. D.; Rossi, G. Macromolecules 1998, 31, 8124.
7. Polishchuk, A. Y.; Valent, A. J. M.; Camino, G.; Luda, M. P.; Madyuskin, N. N.; Lobo, V. M. M.; Zaikov, G. E.; Revellino, M. J Appl Polym Sci 2002, 83, 1157.
8. Hopfenberg, H. B.; Paul, D. R. In Transport Phenomena in Polymer Blends; Paul, D. R.; Newmann, S., Eds.; Academic: New York, 1978; p 445.
9. Wang, C.-L.; Zhao, R.; Cheng, M.-L. J Chem Eng 2001, 15, 521.
10. Yamaguchi, T.; Kuriata, H.; Nakao, S. J Phys Chem B 1999, 103, 1831.
11. Kundu, P. P.; Choudury, R. N. P.; Tripathy, D. K. J Appl Polym Sci 1999, 71, 551.
12. Aminabhavi, T. M.; Phayd, H. T. S.; Ortego, J. D.; Elliff, C.; Rao, A. J Polym Eng 1996, 16, 121.
13. Unnikrishnan, G.; Thomas, S. Polymer 1998, 39, 3933.
14. Unnikrishnan, G.; Thomas, S. J Appl Polym Sci 1996, 60, 963.
15. Unnikrishnan, G.; Thomas, S.; Varghese, S. Polymer 1996, 37, 2687.
16. Sobha, V. N.; Sreekala, M. S.; Unnikrishnan, G.; Johnson, T.; Thomas, S.; Groeninckx, G. J Membr Sci 2000, 177, 1.
17. Harogoppad, S. B.; Aminabhavi, T. M. Polymer 1991, 37, 870.
18. Aminabhavi, T. M.; Phayde, H. T. S. J Appl Polym Sci 1995, 55, 1335.
19. Flory, P. J. Principles of Polymer Chemistry; Cornell University Press: Ithaca, NY, 1953.
20. Unnikrishnan, G.; Thomas, S. J Polym Sci Part B: Polym Phys 1997, 35, 725.
21. Crank, J. The Mathematics of Diffusion; Clarendon Press: Oxford, U.K., 1975.
22. Brown, W. R.; Jenkins, R. B.; Park, G. S. In The Sorption and Diffusion of Small Molecules in Amorphous and Crystalline Polybutadienes; Charles, K. A., Ed.; Interscience: New York, 1973; p 45.
23. Brandrup, J.; Immergut, E. H. Polymer Handbook; Wiley: New York, 1975.
24. Harogoppad, S. B.; Aminabhavi, T. M. J Appl Polym Sci 1991, 42, 2329.
25. George, S. C.; Manfred, K.; Thomas, S. J Membr Sci 1999, 163, 1.
26. Asaletha, R.; Kumaran, M. G.; Thomas, S. Eur Polym J 1999, 35, 253.